JGR Atmospheres

RESEARCH ARTICLE
10.1029/2018JD029301

New Insights on the Impact of Ozone-Depleting Substances on the Brewer-Dobson Circulation

Marta Abalos[1], Lorenzo Polvani[2], Natalia Calvo[1], Douglas Kinnison[3], Felix Ploeger[4,5], William Randel[3], and Susan Solomon[6]

[1]Department of Earth Physics and Astrophysics, Universidad Complutense de Madrid, Madrid, Spain, [2]Department of Applied Physics and Applied Mathematics, Columbia University, New York, NY, USA, [3]National Center for Atmospheric Research, Boulder, CO, USA, [4]Forschungszentrum Jülich, Jülich, Germany, [5]Institute for Atmospheric and Environmental Research, University of Wuppertal, Wuppertal, Germany, [6]Earth, Atmospheric and Planetary Sciences, Massachusetts Institute of Technology, Cambridge, MA, USA

Key Points:
- Increasing ODS have played a key role in observed BDC trends over the last decades of the twentieth century
- Ozone depletion dominates the ODS impact on BDC trends, while the radiative effect of these substances is negligible
- Including changes in mixing in addition to the residual circulation is crucial to interpreting past mean age trends

Supporting Information:
- Supporting Information S1
- Figure S1

Correspondence to:
M. Abalos,
mabalosa@ucm.es

Citation:
Abalos, M., Polvani, L., Calvo, N., Kinnison, D., Ploeger, F., Randel, W., & Solomon, S. (2019). New insights on the impact of ozone-depleting substances on the Brewer-Dobson circulation. *Journal of Geophysical Research: Atmospheres*, *124*. https://doi.org/10.1029/2018JD029301

Received 6 JUL 2018
Accepted 23 JAN 2019
Accepted article online 28 JAN 2019

Abstract It has recently been recognized that, in addition to greenhouse gases, anthropogenic emissions of ozone-depleting substances (ODS) can induce long-term trends in the Brewer-Dobson circulation (BDC). Several studies have shown that a substantial fraction of the residual circulation acceleration over the last decades of the twentieth century can be attributed to increasing ODS. Here the mechanisms of this influence are examined, comparing model runs to reanalysis data and evaluating separately the residual circulation and mixing contributions to the mean age of air trends. The effects of ozone depletion in the Antarctic lower stratosphere are found to dominate the ODS impact on the BDC, while the direct radiative impact of these substances is negligible over the period of study. We find qualitative agreement in austral summer BDC trends between model and reanalysis data and show that ODS are the main driver of both residual circulation and isentropic mixing trends over the last decades of the twentieth century. Moreover, aging by isentropic mixing is shown to play a key role on ODS-driven age of air trends.

Plain Language Summary Concentrations of human-emitted ozone-depleting substances in the stratosphere have increased substantially during the last decades of the twentieth century, which are found in the Southern Hemisphere. These substances have caused stratospheric ozone depletion, which not only has important direct impacts on human health but also leads to important changes in the atmospheric circulation and climate. Here the impact of these substances on the stratospheric mean transport circulation is examined using chemistry-climate model simulations and reanalysis data. In addition to destroying ozone, these substances act as greenhouse gases. In this paper, we find that the radiative forcing impacts of human-emitted ozone-depleting substances on the stratospheric circulation over the last decades of the twentieth century are negligible. In contrast, the Antarctic ozone hole has contributed substantially to the acceleration of stratospheric tracer transport not only in the polar region but globally. The impacts, largest in the austral summer stratosphere, are examined in detail separating the overturning circulation and irreversible mixing. It is shown that trends in the model compare qualitatively well with estimates from two different reanalyses. This paper contributes to advance our understanding of the impact of human emissions on the stratospheric circulation and to untangle the forcings of recent trends.

1. Introduction

The Brewer-Dobson circulation (BDC) transports chemical species in the stratosphere. The term BDC is sometimes used as a synonym of the residual circulation, which is the zonal mean mass transport circulation (e.g., Butchart, 2014). However, it is also frequently used to refer to the net tracer transport circulation, including two-way mixing (e.g., Birner & Bönisch, 2011). In this work, we will use the second terminology to emphasize the important role of mixing in addition to the residual circulation in determining the distribution and variability of tracers in the stratosphere. Note that under this definition, the stratospheric mean age of air (AoA) is directly linked to the BDC strength.

The strengthening of the BDC due to increasing greenhouse gas (GHG) emissions is a robust modeling result (see Butchart, 2014, and references therein). However, these modeled trends have proven hard to detect in the real atmosphere: For instance, insignificant trends in AoA have been reported from long-lived tracer observations in the boreal midlatitude stratosphere (e.g., Engel et al., 2009, 2017). In recent years, however, new studies have found evidence supporting a residual circulation acceleration in the lower stratosphere based on long-term temperature and tracer observations (e.g., Hegglin et al., 2014; Ray et al., 2014; Young et al., 2012), as well as reanalysis data sets (Abalos et al., 2015; Miyazaki et al., 2016). The difficulty in deriving BDC trends can be partly attributed to limited spatial and temporal sampling of the observations, along with the large internal variability in the strength of this circulation (e.g., Garcia et al., 2011; Garfinkel et al., 2017; Hardiman et al., 2017). In addition, because AoA results from integrated effects of residual circulation and mixing, and the latter is also poorly constrained, it is important to assess changes in each of these components of the BDC in order to interpret trends in AoA derived from observations. Overall, it is now generally accepted that there is evidence of an acceleration of the shallow branch of the residual circulation (below ~50 hPa), while larger uncertainty remains in the upper stratosphere.

The observed acceleration of the residual circulation becomes less clear after the year 2000, based on observations of ozone and temperature (Aschmann et al., 2014; Aquila et al., 2016; Randel et al., 2017). Bönisch et al. (2011) highlighted the importance of structural changes in the residual circulation showing decoupled changes in the deep and shallow branches at the beginning of the 21st century. Moreover, the AoA estimates reveal a robust interhemispheric asymmetry in the trends over 2002–2012 (Haenel et al., 2015; Khaykin et al., 2017; Mahieu et al., 2014; Stiller et al., 2012, 2017). It remains unclear what has led to these changes in the trends before and after 2000. Aschmann et al. (2014) argue that a change in tropical sea surface temperatures around the year 1998 explains the recent change in tropical upwelling trends. Stiller et al. (2017) further propose that the decadal variability over 2002–2012 consists in a southward shift of the tropical upwelling region. On the other hand, recent modeling studies have shown that emissions of ozone-depleting substances (ODS) have notably contributed to the past trends in the residual circulation, suggesting that their decrease starting at the beginning of the 21st century may explain the weakening of the trends (Aquila et al., 2016, Polvani et al., 2017, 2018).

The impact of the ODS on the BDC trends has been addressed in a number of papers (e.g., Garfinkel et al., 2017; Keeble et al., 2014; Li et al., 2008; McLandress et al., 2010; Oberländer et al., 2013; Oman et al., 2009; Oberländer-Hayn et al., 2015; Polvani et al., 2018). These works have shown that Antarctic ozone depletion is the main driver of the residual circulation acceleration in the Southern Hemisphere (SH) summer over the last several decades of the twentieth century in various chemistry-climate models. Unlike some previous studies that treat ozone as a forcing, here we emphasize that the external forcing to be compared to GHG are the man-made ODS emissions, since stratospheric ozone is naturally abundant and not an anthropogenic emission like GHG. This distinction between impacts of ozone and impacts of ODS is important because, in addition to causing ozone depletion, ODS have a direct climate warming effect. We refer to the former as the *chemical* and to the latter as the *radiative* impacts of the ODS on the BDC.

On one hand, the increases in ODS over the last decades of the twentieth century have caused the Antarctic ozone hole to form, with first-order impacts on radiative balances, temperature, and circulation in the austral lower stratosphere spring and summer (see Thompson et al., 2011; Previdi & Polvani, 2014, for recent reviews). The induced dynamical changes in the austral summer lower stratosphere include an acceleration of the zonal mean wind, which delays the polar vortex breakdown (e.g., Orr et al., 2013; Son et al., 2010). These changes in turn drive trends in the wave drag and consequently in the BDC, and previous modeling works have shown an acceleration of the SH polar downwelling in December-January-February (DJF) associated with the Antarctic ozone hole (e.g., Polvani et al., 2018). However, because trends in AoA and chemical tracers result from a combination of changes in residual circulation and isentropic mixing, it is important to evaluate changes in these separate contributions.

On the other hand, some studies have examined the importance of the warming effect of ODS in terms of the future global warming that would have been expected if the Montreal Protocol had not been implemented (Garcia et al., 2012; Newman et al., 2009). These works refer to this future scenario as the *World Avoided* and find a climate impact of ODS comparable to other GHG toward the end of the 21st century. Focusing on the past impacts of the already-emitted ODS, McLandress et al. (2014) performed sensitivity runs to evaluate the radiative impact of ODS (halocarbons) and found an acceleration of the tropical upwelling of about half that due to CO_2 emissions over the period 1960–2010. To our knowledge, there are no other studies on the radiative impacts of ODS over past decades.

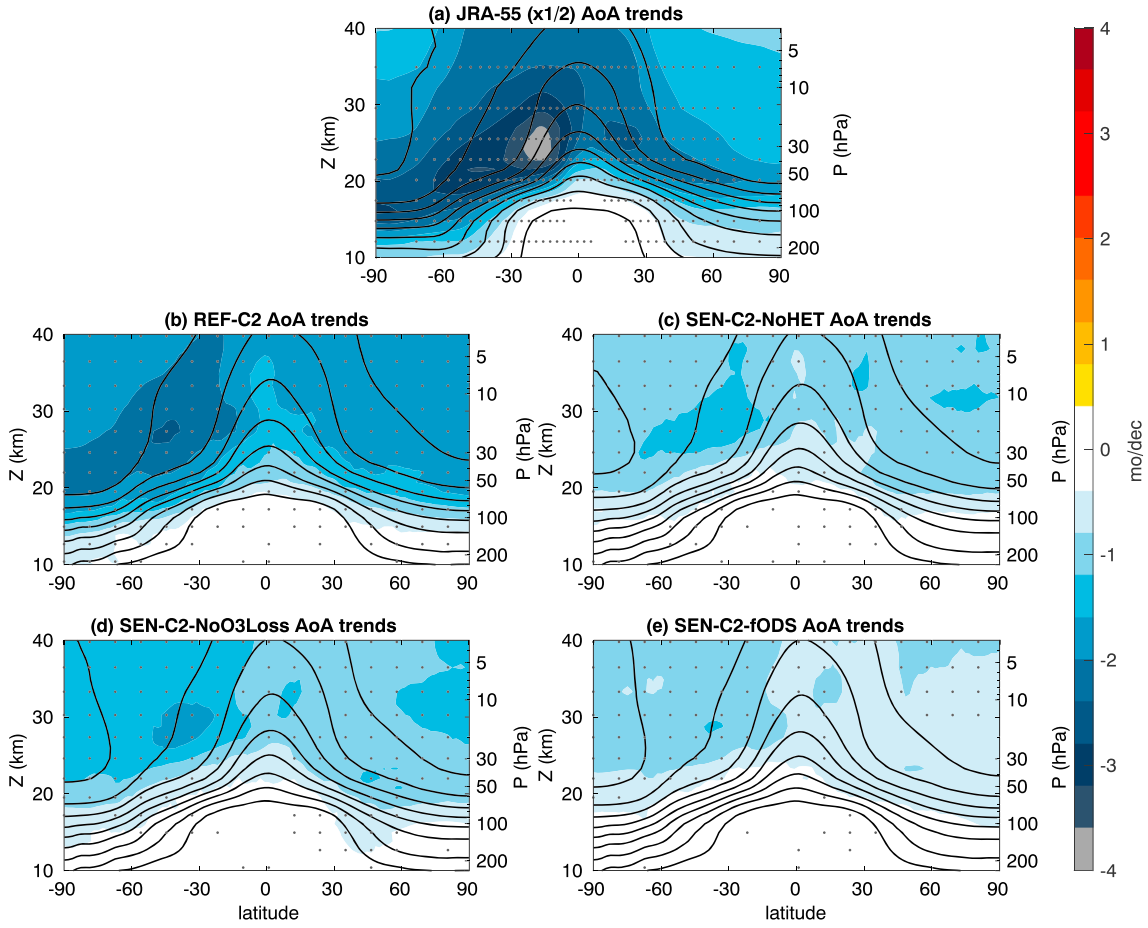

Figure 1. Trends in annual mean AoA for JRA-55 (a, values in color scale need to be multiplied by 2 to obtain trends) and the ensemble mean of model runs: control run (REF-C2; b), sensitivity runs SEN-C2-NoHET (c), SEN-C2-NoO3Loss (d), and SEN-C2-fODS (e). The trends in the reanalyses are computed over 1980–2000, while for the model runs over 1970–2000. Black contours show the climatology with contour interval 6 months. Dots denote statistically significant trends at the 95% level.

The focus of this paper is an explicit evaluation of the ODS influence on the observed BDC trends over the last decades of the twentieth century, based on sensitivity model simulations and comparison with reanalysis data. Section 2 describes the model and reanalysis data sets used. Section 3 compares the relative roles of the radiative versus chemical (i.e., ozone depletion) pathways of ODS influence on BDC trends. Section 4 examines the impact of the ODS on the austral summer BDC trends, analyzing changes in both the residual circulation and isentropic mixing. Section 5 summarizes the main results and discusses their implications.

2. Data and Methods

2.1. Reanalysis Data

The Japanese Re-Analysis (JRA-55) is used for comparison to model results. This reanalysis is particularly useful for the present study because, unlike other reanalyses such as European Centre for Medium-range Weather Forecasts Interim Re-Analysis (ERA-Interim), the underlying model has time-dependent ozone from 1979 onward, obtained from a separate chemistry-climate model run nudged to meteorological fields (which impacts the dynamics through the radiative scheme; see Kobayashi et al., 2015). This implies that the ozone-dynamics interactions are represented more accurately than in other reanalyses, which use an ozone climatology in the radiative scheme (e.g., ERA-Interim). This reanalysis is available continuously from 1958 to the present, but here we focus on the period 1980–2000 for which we have AoA data available. This period is also that of strongest ozone depletion impacts on the BDC. The robustness of trends seen in the JRA-55 reanalysis is briefly discussed in section 5 comparing to the ERA-Interim (Dee et al., 2011) for the period 1980–2000. The AoA for these reanalyses is obtained from simulations with the Chemical Lagrangian

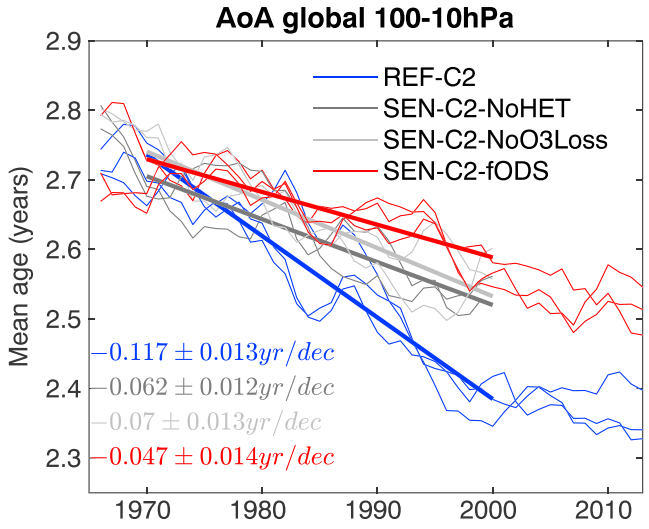

Figure 2. Time series of annual mean AoA averaged globally over 100–10 hPa for the reference and sensitivity runs. All series are smoothed with a 3-point running mean. Thin lines are the ensemble members. Straight lines show the linear fit of the ensemble mean over 1970–2000: solid if statistically significant and dashed otherwise.

Model of the Stratosphere (e.g., Ploeger & Birner, 2016) with transport based on 3-D diabatic trajectories and a parameterization of small-scale mixing that depends on deformations in the large-scale flow.

2.2. WACCM Simulations

We use model runs of the Community Earth System Model, version 1 (CESM1) using the Whole Atmosphere Community Climate Model (WACCM), version 4, as the atmospheric component. The model version is based on CAM4 (Neale et al., 2013). The chemistry module is an update to (Kinnison et al., 2007) the Chemistry Climate Model Initiative (CCMI, ; Eyring et al., 2013, Morgenstern et al., 2017). WACCM extends to nearly 140 km and has 66 vertical levels, a horizontal resolution of 2.5° longitude by 1.9° latitude, and a vertical resolution of 1.2–1.5 km in the lower stratosphere. Marsh et al. (2013) provide further information of the version of the model used here, and more recent modifications to the gravity wave parameterization are described in Garcia et al. (2017). This version of the model does not generate an internal Quasi-Biennial Oscillation, which is here included by nudging the equatorial winds to observations.

We analyze model runs covering the historical period 1960–2013, all carried out with the fully coupled model (atmosphere, ocean, ice, and land components active). The analyses are based on two different types of runs with different forcings: the control runs including all forcings, which are the CCMI reference runs denoted REF-C2, and the sensitivity runs also carried out for CCMI denoted SEN-C2-fODS, which are exactly equal to the reference runs except in that the ODS emissions are fixed at year 1960 values (pre-ozone hole). There are three members for each of the run setups, REF-C2 and SEN-C2-fODS. We consider the ensemble mean trends of each run setup in order to reduce internal variability and capture the forced response. The difference between ensemble means of the control run minus the sensitivity run provides the *Impact of ODS*, since the presence of these substances is the only difference between the two.

In addition to these CCMI runs, two more sensitivity runs are carried out in order to separate the radiative from the chemical (ozone depletion) ODS impact on BDC, covering 1960–2000. These include time-varying concentrations of ODS, constrained in such a way that these substances do not cause ozone depletion. Hence, by construction, these runs include the radiative impacts of ODS but not the chemical impacts. Two types are distinguished: the SEN-C2-NoHET and the SEN-C2-NoO3Loss. In the runs denoted SEN-C2-NoHET, all heterogeneous reactions leading to chlorine activation have been shut down. This ensures that, although ODS are present in the atmosphere and thus have a radiative impact, ozone depletion in the lower stratosphere (notably the Antarctic ozone hole) is not occurring (Solomon et al., 1986). In addition to these heterogeneous reactions responsible for ozone depletion in the lower stratosphere, gas phase chemistry destroys ozone in the upper stratosphere (Molina & Rowland, 1974). To test the importance of the impact of gas-phase ozone depletion in the upper stratosphere on the BDC, the SEN-C2-NoO3Loss are performed. These have time-varying ODS concentrations but both heterogeneous ozone loss and rate-limiting gas-phase reaction reaction $ClO + O \rightarrow O_2 + Cl$ are shut down. Two members of each of these two additional run setups (SEN-C2-NoHET and SEN-C2-NoO3Loss) are performed.

3. Chemical Versus Radiative Impacts of ODS on the BDC

Analyzing some of the WACCM runs described above (REF-C2 and SEN-C2-fODS), Polvani et al. (2018) have shown that ODS and GHG have had comparable impacts in driving the modeled global BDC acceleration over the last decades of the twentieth century: Approximately half of the global AoA trends in WACCM over 1960–2000 were caused by ODS. In addition, they highlight that ODS alone can explain the strong acceleration of the polar downwelling in the SH summer lower stratosphere. Thus, they identified both global and regional impacts of ODS on the BDC. However, the question of whether these effects are attributed exclusively to ozone depletion or if the radiative effect of ODS is contributing significantly was not addressed in that study. In this section, we explore these different impacts by comparing the model runs used in Polvani et al. (2018) to the additional sensitivity runs without ozone depletion introduced in section 2.2.

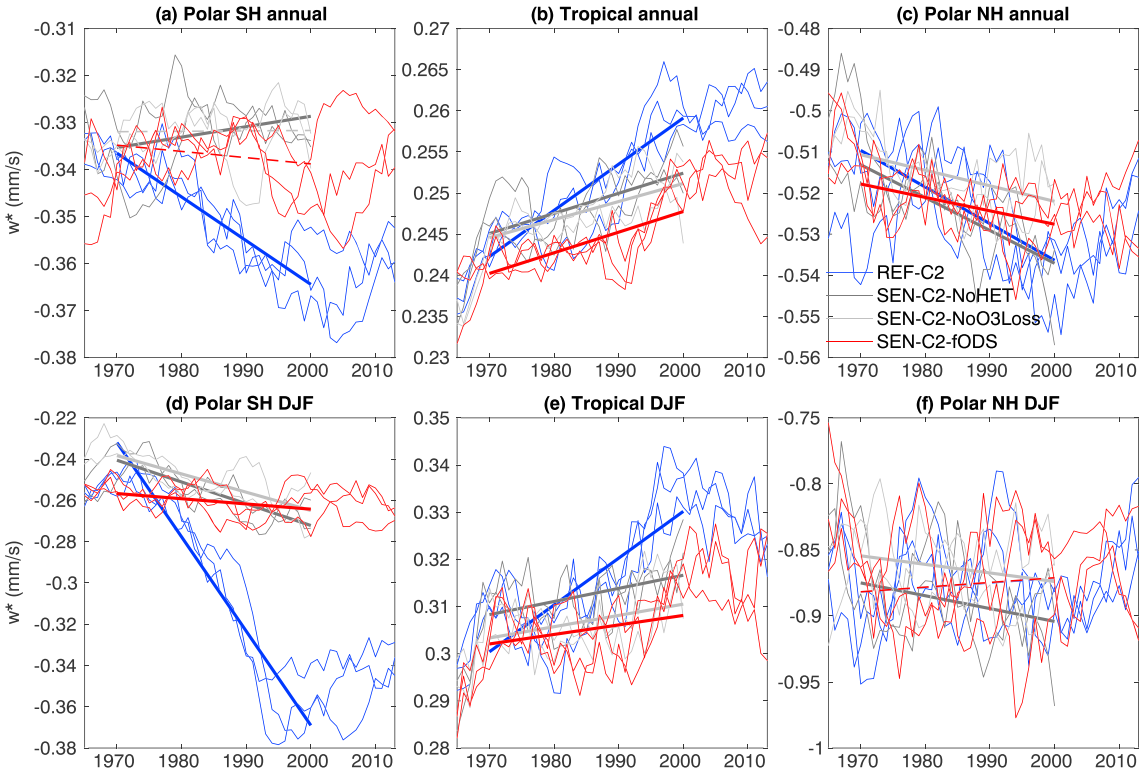

Figure 3. Time series of 70-hPa annual (a–c) and DJF (d–f) residual circulation vertical velocity in the SH polar region (a and d; 60–90S), tropics (b and e; 30S to 30N) and NH pole (c and f; 60–90N), for the reference and sensitivity runs. Thin lines are the ensemble members. All series are smoothed with a 7-point running mean. Straight lines show the linear fit of the ensemble mean over 1970–2000: solid if statistically significant and dashed otherwise.

Figure 1 shows the annual mean AoA trends in the JRA-55 reanalysis and the ensemble mean of the WACCM runs over the period 1980–2000. The first thing to note is that AoA trends in JRA-55 are negative throughout the domain, indicating an acceleration of the residual circulation (Figure 1a). However, this is not necessarily the case for other reanalyses (e.g., Diallo et al., 2012, Ploeger et al., 2015). The recent paper by Chabrillat et al. (2018) compares the AoA in five modern reanalyses and finds substantial differences in the linear trends for the period 1989–2001. Hence, uncertainties in BDC trends derived from reanalysis are large, and this issue will be further addressed in section 5. For now, considering the reasons for using JRA-55 given in section 2 and for the sake of comparing to our model results, we focus on this specific reanalysis as a useful estimate of the real atmosphere.

The AoA trends in the model control run REF-C2 (Figure 1b) are also negative throughout the stratosphere and show a similar spatial structure to those in JRA-55, with stronger negative values over most of the SH stratosphere. However, the JRA-55 trends are more than 4 times larger than those in the model in the global average (note that in Figure 1a the trends are divided by 2 in order to plot them with the same color scale as the model results). This is partly due to the fact that the climatological values of AoA are about 0.5 to 1 year older in the reanalysis than in the model in the lower stratosphere (not shown; differences are smaller at higher levels). We note that AoA is defined from a reference point at 139 hPa in the tropics in WACCM and at the surface in Chemical Lagrangian Model of the Stratosphere. Although this might explain a small fraction of the difference in the climatologies, it likely does not play a role in the trends. In relative terms (dividing by the climatology) the trends are still twice as large in the reanalysis as in the model for the global mean. We note that this difference is also seen when the same period is considered for model and reanalysis (1980–2000).

Figures 1c–1e show that ODS contribute significantly to the global AoA decrease over the period, since the sensitivity runs show much smaller trends than the control run. The agreement between the AoA trends in the three sensitivity runs demonstrates that heterogeneous chemical ozone depletion is mainly responsible for the ODS impact on the BDC. Specifically, the fact that AoA trends in the SEN-C2-NoO3Loss, where the radiative impact of ODS is included, are similar to those in SEN-C2-fODS, where ODS increases are not

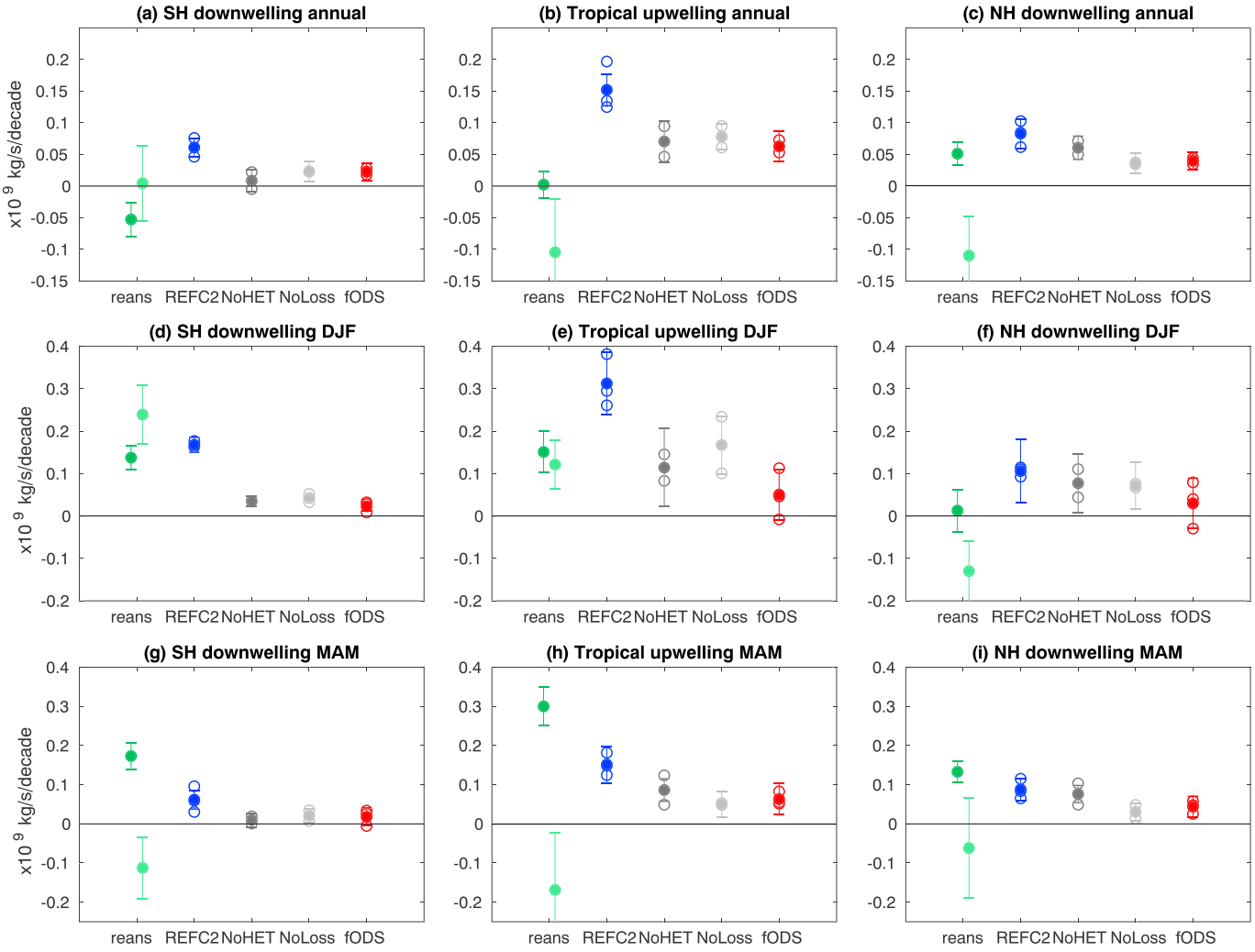

Figure 4. Trends at 70 hPa over 1970–2000 in net upward (b, e, and h) and downward mass flux in each hemisphere (SH [a, d, and g] and NH [c, f, and i]) for the annual mean (a–c), DJF (d–f), and MAM (g–i). Two reanalyses are shown in green (dark: JRA-55, light: EI), control runs (REF-C2) in blue, SEN-C2-NoHET in dark gray, SEN-C2-NoO3Loss in light gray, and SEN-C2-fODS in red. Note that for EI the trends are computed over 1979–2000. The trends are computed after applying a 7-point running mean to the time series. For the model runs, all ensemble members are shown in circles, and filled circles show the ensemble mean trends. Error bars represent the statistical significance of the ensemble mean trends at the 95% level from a Student *t* test.

present at all (concentrations are fixed at 1960 levels), implies that the radiative impact of ODS on the AoA is negligible. Moreover, the similarity between the SEN-C2-NoO3Loss and SEN-C2-NoHET sensitivity runs reveals that there is little influence of the gas-phase chemistry on the BDC trends.

To quantify the different ODS impact on the AoA trends in the different model setups, Figure 2 shows the time series of AoA area-averaged globally between 100 and 10 hPa for all the model runs and displays the trend values. Consistent with the results of Polvani et al. (2018), we observe a substantial (about 60%) reduction of the trends from the control run (blue) to the fixed ODS run (red). In addition, the gray lines also show a significantly smaller slope than the control run (about 47% and 40% reduction for the SEN-C2-NoHET and SEN-C2-NoO3Loss runs, respectively). This confirms that changes in ozone depletion, which are suppressed in these sensitivity runs, are the main cause for the slope reduction. In particular, the trends in the three sensitivity runs are indistinguishible within uncertainties and around 50% smaller than those in the control runs.

It is well known that the AoA integrates transport throughout the stratosphere, with contributions from both local and remote changes. Since most air mass enters the stratosphere through the tropical tropopause, the strength of upwelling in this region is key for the global AoA. In fact, lower stratosphere tropical upwelling is

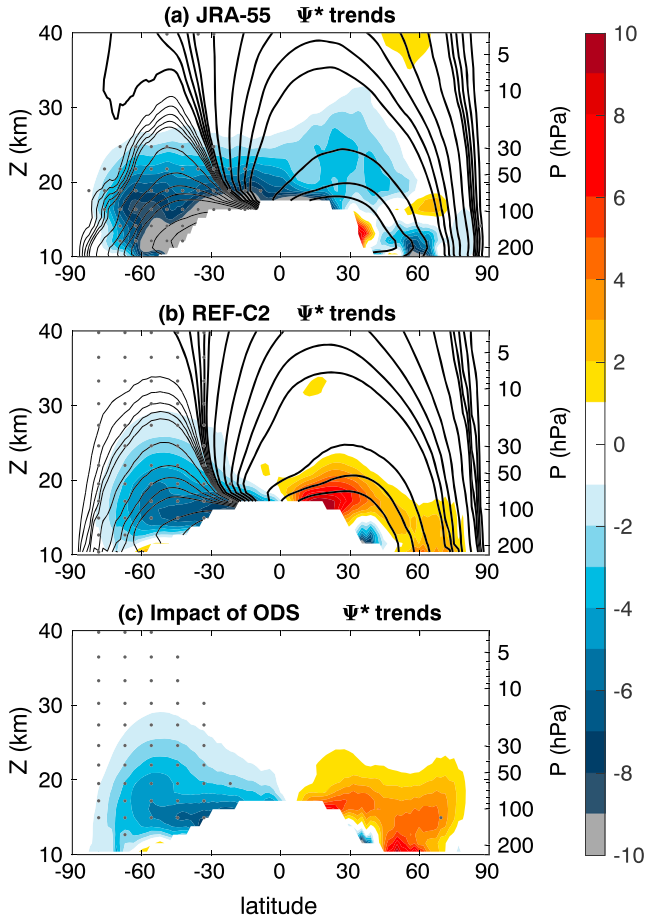

Figure 5. Residual stream function trends (shading, in kg · m^{-1} · s^{-1}) and climatology (contours) in DJF over the period 1980–2000 for (a) JRA-55, (b) the ensemble mean control run REF-C1, and (c) the impact of ODS (difference REF-C2 minus SEN-C2-fODS). Black contours in (a) and (b) show the climatology, with thin contours indicating negative values. Contours: ±1:5, 10:10:50, 50:50:200 kg · m^{-1} · s^{-1}. Dots denote statistically significant trends at the 95% level.

commonly used to evaluate the BDC response to global warming. On the other hand, the interhemispheric asymmetry in the AoA trends seen in Figures 1a and 1b suggests a localized impact of Antarctic ozone depletion. In order to evaluate these changes separately, Figure 3 shows time series of tropical upwelling and polar downwelling in each hemisphere. Consistent with the above statements, the behavior of tropical upwelling (Figure 3b) is similar to that of AoA, with all sensitivity runs showing similar trends, smaller than the reference run. The strongest impact of ODS is seen in the SH polar stratosphere (Figure 3a), where all sensitivity runs fail to capture the acceleration of polar downwelling. In contrast, no clear distinction between the control and sensitivity runs can be detected in the Northern Hemisphere (NH) polar stratosphere (Figure 3c). As found in Polvani et al. (2018), the annual mean signal is dominated by the trends in DJF, both in tropical upwelling and SH polar downwelling (Figures 3d–3f). The novelty of the results in Figure 3 with respect to that previous work is that here ozone depletion is explicitly identified via the sensitivity runs as the main factor responsible for the ODS impact on residual circulation trends. This implies that, at least in WACCM, the greenhouse effect of ODS does not play a significant role in the past residual circulation trends.

While it is well understood that the ozone hole drives an acceleration of downwelling in austral summer, the remote influence of this seasonally and regionally localized feature on tropical annual mean upwelling is not straightforward. Note that, although residual vertical velocities are comparable for polar downwelling and tropical upwelling (see Figure 3), the net mass flux is smaller across the polar region due to its reduced area. This difference is especially large in the SH summer season downwelling, since most of the air mass rising in the tropics is transported into the NH (winter hemisphere). Hence, the question is whether the SH summer polar stratospheric downwelling is able to modify tropical upwelling by mass continuity or if

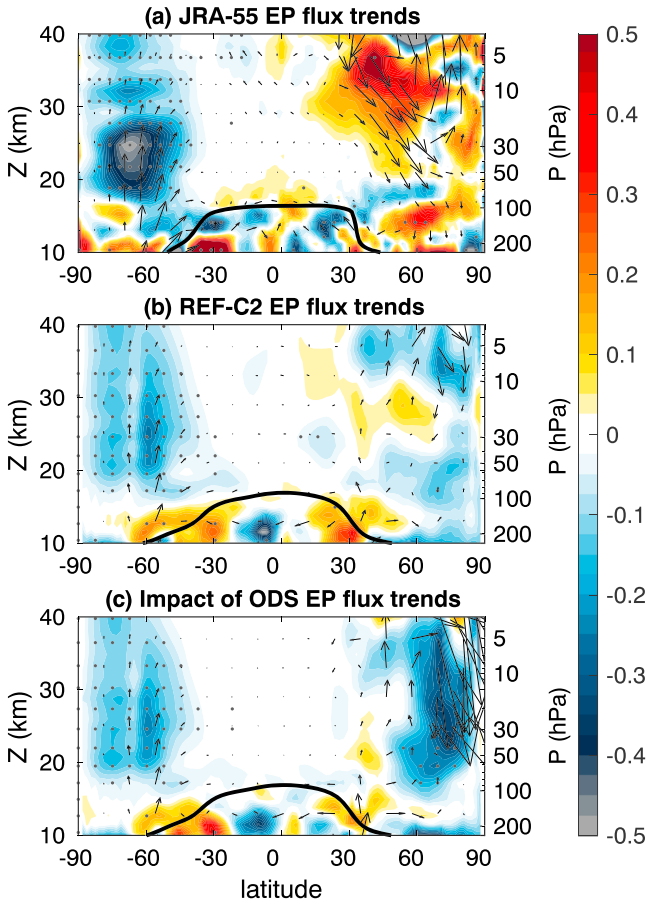

Figure 6. Trends in EP flux (arrows) and its divergence (shading) in DJF over the period 1980–2000 for (a) JRA-55, (b) the control run REF-C1, and (c) the impact of ODS (difference REF-C2 minus SEN-C2-fODS). The black thick line shows the tropopause. Dots denote statistically significant trends of the EP flux divergence at the 95% level.

this signal survives the annual average. To address this question, Figure 4 shows trends in net upward mass flux (integrated over turnaround latitudes, i.e., over the entire region of upwelling for each month) and net downward mass flux in each hemisphere at 70 hPa, for the annual mean, DJF and March-April-May (MAM) (the other two seasons do not show a significant impact of ODS). The trends in SH downwelling in DJF (Figure 4d) stand out as the most robust difference between the reference and the sensitivity runs. This difference is reflected in the tropical upwelling mass flux (Figure 4e), although there are much larger uncertainty bars, which are linked to NH downwelling (Figure 4f). This DJF response is mirrored in the annual mean trends (Figures 4a–4c), although the net southern hemispheric mass flux shows a much more modest annual mean reduction than the polar downwelling alone (compare Figures 3a and 4a). In MAM, there is a slight reduction of the upwelling mass flux trends in the sensitivity runs as compared to the control run. This could imply a contributing role from Arctic ozone depletion to the annual mean global response, although this effect is much less robust than the Antarctic ozone hole effect (compare Figures 4d to 4i).

The good correspondence between the fixed ODS and the other two sensitivity runs seen in Figures 1 –4 implies that the ODS impact is dominated by the effect of the Antarctic ozone hole, and this is true not only for the DJF SH downwelling but also for the annual mean net upwelling mass flux. Figure 4 also shows the mass flux trends in the reanalysis JRA-55 and EI for comparison (note that EI trends are computed over a shorter period due to data availability). Consistent with previous studies (e.g., Abalos et al., 2015), the trends in the two reanalyses do not always agree (e.g., in the tropical upwelling annual mean trends, Figure 4b). Here we show that the agreement with the model trends is also limited. An important exception is found in austral summer (Figure 4d), which shows notably good agreement between the model and the

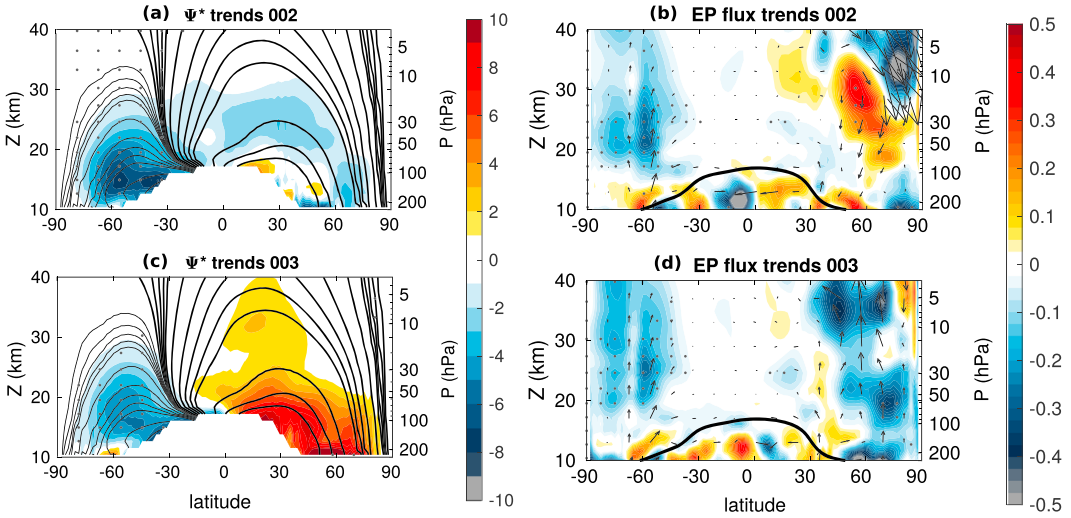

Figure 7. Residual stream function (a, c) and EP flux (b, d) trends for the control run REF-C2 for two different members (a and b, member 1; c and d, member 2). In (a) and (c), black contours show the climatology, with negative values thinner (contour values as in Figure 5). In (b) and (d), the shading shows the EP flux divergence and arrows the EP flux. Dots denote statistically significant trends at the 95% level.

two reanalyses. The robustness of this signal and the fact that DJF shows the largest impact of ODS motivates us to investigate the trends in this season more in detail in the next section.

4. Antarctic Ozone Depletion Impact on the BDC

As mentioned in the section 1, the BDC includes residual circulation and mixing. In this section, we evaluate the trends in each component and the contributions to AoA focusing on the period of strongest Antarctic ozone depletion 1980–2000 (e.g., Solomon et al., 2016).

Figure 5 shows trends in the residual circulation streamfunction in the reanalysis JRA-55 and the model. The reanalysis and model trends (Figures 5a and 5b) show similar acceleration cells of the residual circulation in the SH, although stronger in JRA-55 than in the model below 20 km. In Figure 5c, much of this feature is explicitly attributed to ODS, and in particular to their chemical impact through ozone depletion (as demonstrated in the previous section). Figure 6 shows that this acceleration of the SH residual circulation is driven by stronger Eliassen-Palm (EP) flux convergence resulting from enhanced upward wave propagation into the stratosphere in the SH middle and high latitudes. Comparing Figures 6b and 6c, it is clear that the stronger convergence is entirely associated with ODS emissions. These trends in wave propagation are associated with the westerly zonal wind trends induced by polar cooling linked to the ozone hole.

In Figures 5 and 6, it is evident that, while there is good agreement between the model ensemble mean and reanalysis on the acceleration in the SH lower stratosphere, trends in the NH do not agree. Note that these trends are not statistically significant in neither reanalysis nor model. This points to the important distinction between the internal climate variability present in the observations and also in each of the three runs, and the forced response which is more clearly identified by the ensemble mean of the three members. These comparisons suggest that the reanalysis trends in the NH are not a forced response but mainly reflect internal climate variability. To illustrate this point, Figure 7 shows the trends in residual circulation and EP flux for two members. It is clear that different members have different behavior in the NH, but all show consistent trends in the SH.

The enhanced SH EP flux convergence in Figure 6 not only drives a stronger residual circulation but also can potentially lead to changes in isentropic mixing, which is a fundamental component of stratospheric transport (e.g., Plumb, 2002). To quantify changes in isentropic mixing, we have computed the normalized equivalent length squared Λ_{eq}, which is proportional to effective diffusivity, an accurate estimate of the mixing based on contour elongation of a conserved tracer on isentropes (Haynes & Shuckburgh, 2000). Specifically, we used potential vorticity as an approximately conserved tracer in these calculations, which is a reasonable approximation in this region as shown in Abalos et al. (2016). Figure 8 shows the trends in

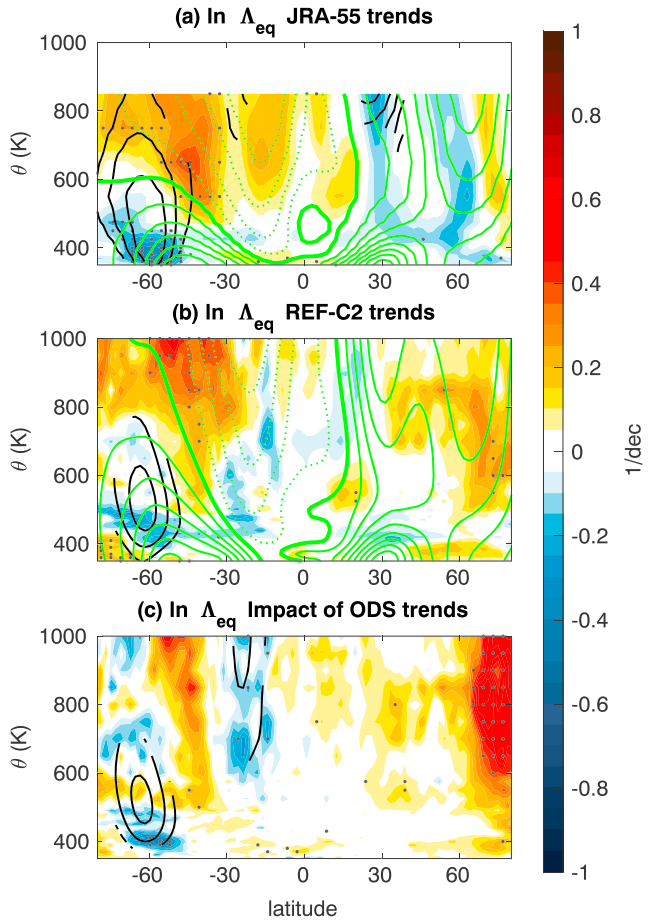

Figure 8. Normalized equivalent length squared Λ_{eq} trends in DJF over the period 1980–2000 (shading) for (a) JRA-55, (b) REF-C2 control run, and (c) impact of ODS (difference REF-C2 minus SEN-C2-fODS). Dots denote statistically significant trends at the 95% level. Black contours indicate westerly wind trends (only statistically significant trends are plotted). Contour interval for the zonal wind trends is 0.6 m/s per decade, zero contour omitted. Green contours in (a) and (b) show the climatological values of zonal wind with 5 m · s^{-1} contour intervals, and zero contour is thicker.

equivalent length, with zonal wind trends overlaid as black contours. Reanalysis and model show consistent patterns in the SH, with weaker mixing in the polar lower stratosphere (~400–500 K) and stronger mixing above and equatorward of the region of westerly wind trends. Note that we have interpolated potential vorticity in the reanalysis to the coarser model resolution in order to make a quantitative comparison of the Λ_{eq} results. The enhanced isentropic mixing in the model extends to higher altitude than in JRA-55. This is related to the different background zonal wind climatology, shown by the green contours: The zero wind line extends to higher levels in WACCM (~1000 K) than in the reanalysis (~600 K). Too strong DJF westerlies in the SH polar stratosphere is a common model bias probably linked to missing gravity wave drag (e.g., de la Cámara et al., 2016). The isentropic mixing trends seen in JRA-55 and in the model imply an upward shift in the region of isentropic mixing due to the enhanced EP flux propagation into the stratosphere (Figure 6). Our sensitivity runs with fixed ODS demonstrate that the observed trends in austral winter isentropic mixing are caused by the ozone hole, as previously hypothesized in Abalos et al. (2016).

Given that transport timescales in the stratosphere (i.e., AoA) depend on both the residual circulation and isentropic mixing, the net impact of the ozone hole on the AoA in austral summer is not clear a priori. Faster residual circulation (Figure 5) leads to smaller AoA in the lower stratosphere, but the reduction in isentropic mixing (Figure 8) will tend to increase AoA in this region. Figure 9 shows the DJF trends in AoA for the reanalysis and model, and the impact of ODS. While the global mean trends are negative, one can see a region of positive trends in the Antarctic lowermost stratosphere in the model. This has been noted recently in several CCMI models and identified as an ODS-driven feature (Li et al., 2018; Morgenstern et al., 2018). Interestingly, the reanalysis shows a region of weaker negative trends (not reaching positive values)

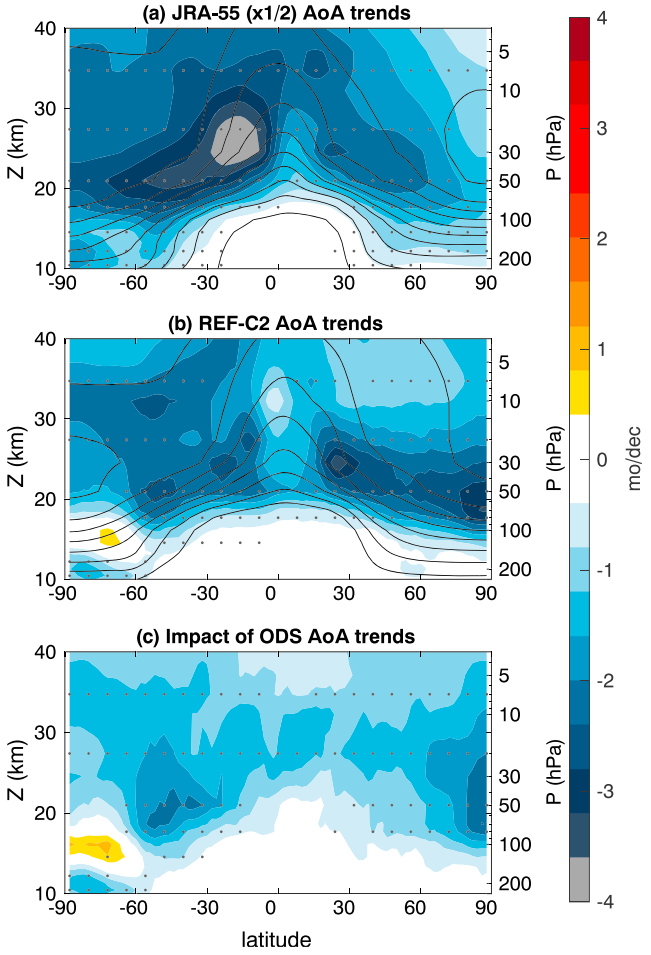

Figure 9. AoA trends in DJF over the period 1980–2000 for JRA-55 (a, values in color scale need to be multiplied by 2 to obtain trends) and model runs. (b) Ensemble mean of control runs (REF-C2) and (c) impact of ODS (difference REF-C2 minus SEN-C2-fODS ensemble means). Black contours in (a) and (b) show the climatology with contour interval 6 months.

over that same region (60–90S, 10–20 km). These results suggest that effects of the reduced mixing dominate over those of the strengthened overturning circulation in the model but are of similar magnitude in the reanalysis.

The contributions to the total mean age can be explicitly estimated by calculating the Residual Circulation Transient Timescale (RCTT) and aging by mixing (Birner & Bönisch, 2011; Garny et al., 2014). The aging by mixing can be derived to a first approximation by subtracting the RCTT from the AoA, although this includes both resolved and numerical diffusion (Dietmüller et al., 2017; Ploeger et al., 2015). Figure 10 shows contributions to the DJF trends in AoA from RCTT and aging by mixing, for the JRA-55 reanalysis and the model ensemble mean. This decomposition clearly identifies the positive AoA trends in the SH polar lower stratosphere with aging by mixing, confirming the previous suggestion by Li et al. (2018). Interestingly, the midlatitude AoA negative trends in the annual mean (Figure 1) are also dominated by aging due to mixing (see Figure S1 in the supporting information). It is important to note that changes in aging by mixing do not only account for trends in local mixing efficiency (seen in equivalent length, Figure 8), but, because it is a Lagrangian integrated measure, it may also include changes in residual circulation trajectories (Ploeger et al., 2015). In other words, even with constant mixing efficiency of the flow at each latitude and altitude, air parcels can experience different degree of mixing because the location or speed of the residual circulation trajectories has changed. In addition, the role of aging by mixing could be overly emphasized by our assumption of negligible numerical diffusion, as this term is likely nonnegligible (Dietmüller et al., 2017).

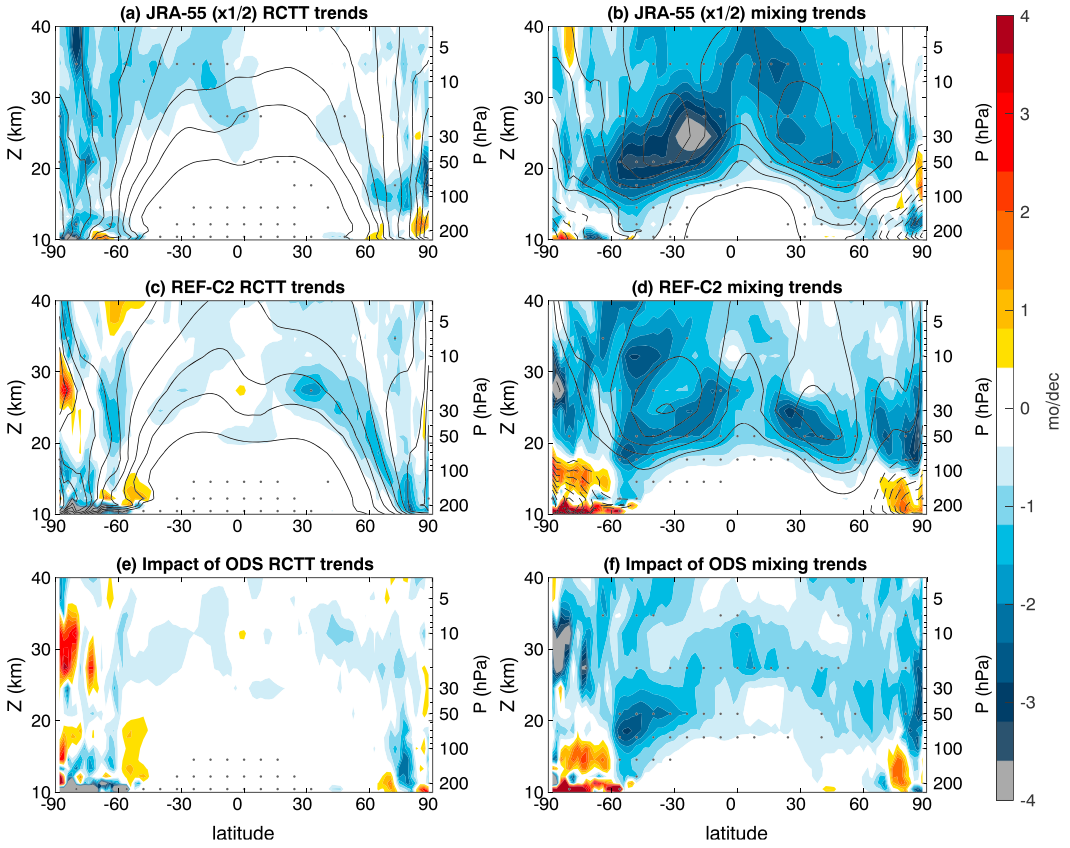

Figure 10. Trends over 1980–2000 in DJF RCTT (a, c, e) and aging by mixing (b, d, f) for JRA-55 (a and b, values in color scale need to be multiplied by 2 to obtain trends) and model runs. (c, d) Control run (REF-C2). (e, f) Impact of ODS (difference REF-C2 minus SEN-C2-fODS). Black contours in (a)–(d) show the climatology with contour interval 6 months.

However, it is clear from Figures 10 and S1 that changes in residual circulation strength alone cannot explain the AoA trends over the period of study, and changes in mixing are important.

Finally, to demonstrate that the timing of the AoA trends over the Antarctic is related to the delayed polar vortex breakup, Figure 11 shows the time evolution of AoA, RCTT, and aging by mixing trends in the polar austral stratosphere from September to May. Again, we see a consistent behavior in the reanalysis and the model, with a propagation of the positive (near zero for JRA-55) AoA trends over time to lower levels, closely following the aging by mixing trends. These positive AoA trends coincide with the period when the climatological AoA is decreasing (as shown by the upward slope of the AoA contours) due to the transition from winter to summer stratospheric circulation regime. The ozone hole and thus ODS-driven westerly trends delay this transition in the lower stratosphere by inhibiting two-way mixing of younger air from midlatitudes into the polar region (Figures 11c, 11f, and 11i). The positive trends in aging by mixing in the reanalysis are weaker and confined to lower levels than in the model, resulting in near-zero AoA trends.

5. Conclusions and Discussion

This work builds upon previous studies that have examined the impacts of ODS on the BDC and confirms that ODS have played a major role on the observed BDC trends over the last decades of the twentieth century, especially in DJF SH. One important novelty of this study is that it presents the first comparison of the BDC trends between reanalysis data and a chemistry-climate model with the focus of identifying the ODS impact. The ODS signal is obtained via model sensitivity runs with ODS emissions fixed to pre-ozone hole levels (year 1960). We have compared JRA-55 with the WACCM model and found qualitatively good agreement; however, quantitatively the relative AoA trends are approximately twice as large in the reanalysis than in the model ensemble mean. We emphasize that there are substantial differences among reanalyses on the BDC trends and the choice of JRA-55 in this work is motivated by the accurate representation of ozone-climate

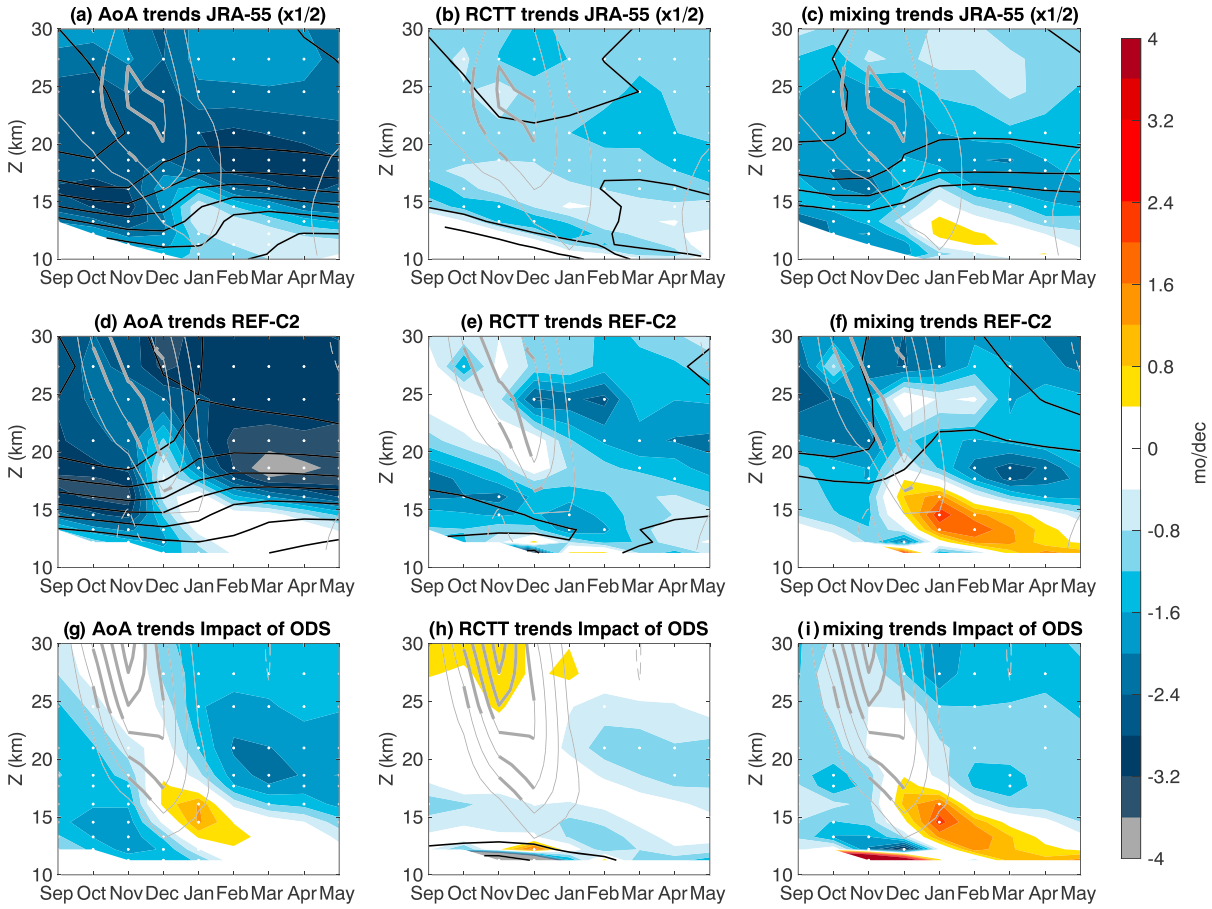

Figure 11. Trends in AoA (a, d, g), RCTT (b, e, h) and aging by mixing (c, f, i) in the Southern Hemisphere polar (90–60S) stratosphere as a function of month of the year (September–March) and log-pressure altitude. (a–c) JRA-55 (divided by 2). (d–f) Control runs. (g–i) Impact of ODS (difference REF-C2 minus SEN-C2-fODS). Black contours in (a)–(f) show the climatology with contour interval of 6 months. Contour interval for the zonal wind trends is 1 m/s per decade, zero contour omitted.

interactions in this reanalysis and the fact that it extends further back in time than others. Nevertheless, Figures 12a and 12b show that the DJF trends obtained for JRA-55 residual circulation and isentropic mixing over the period 1980–2000 are qualitatively consistent with those found in ERA-Interim indicating that these are robust features present in the observations. Larger uncertainties exist in the AoA trends, which do not show negative trends in the SH over the period 1980–2000 (not shown). However, the expected negative SH AoA trends appear also in ERA-Interim when the period is slightly modified (to 1984–2000; Figure 12c). In contrast, the NH trends have opposite sign in both reanalyses. This discrepancy in AoA trends is consistent with the recent results of Chabrillat et al. (2018) for 1989–2001, despite the different periods and AoA calculations (based on diabatic transport model here and on kinematic transport model in Chabrillat et al., 2018). Here we show that, despite large discrepancies in BDC trends among reanalyses pointed out in previous works, the trends over the region and period of the Antarctic ozone hole are robust. Furthermore, given the consistency between the reanalysis and the model (which is internally balanced), we argue that these austral summer BDC trend features can be regarded as benchmarks that should be captured by other reanalyses.

A second important result of this study is the distinction between the chemical (i.e., ozone depletion) and the radiative pathways of the ODS impact on the BDC trends by performing sensitivity runs in which ODS are present but do not deplete ozone. The results show that the radiative impact of ODS does not play a significant role in driving BDC trends over the last decades of the twentieth century. Moreover, the Antarctic ozone hole in the lower stratosphere is identified as the main responsible for ODS-driven BDC trends. The connection between this regionally and seasonally confined feature and the global mean BDC is found in

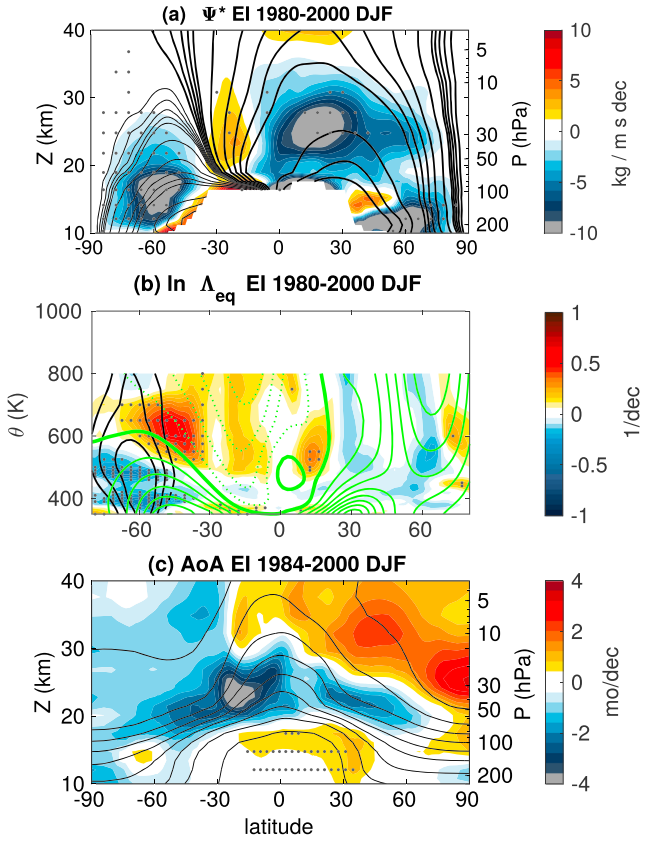

Figure 12. Trends for EI in DJF (a) residual circulation over 1980–2000, (b) equivalent length over 1980–2000, and (c) mean age of air over 1984–2000. In (a), black contours show climatology as in Figure 5. In (b), black contours show the zonal wind trends and green contours show the climatological values of zonal wind, with the same contour intervals as Figure 8. In (c), black contours show climatological values with the same contour interval as in Figure 9.

the lower stratosphere tropical upwelling. The ozone hole accelerates residual circulation in the austral summer hemisphere by changing the wave propagation conditions (Figures 5 and 6). By mass continuity tropical uwpelling is accelerated, and this DJF impact dominates the annual mean response (Figures 4d and 4e). While this negligible role of the radiative pathway of ODS is in contrast with the results of (McLandress et al., 2014), it is consistent with the radiative forcing of chlorofluorocarbons being only about 14% of that of CO_2 from 1759 to 2011 (Myhre & Shindell, 2013). A possible reason for the discrepancy with McLandress et al. (2014) is that in that work the heating rates due to halocarbons were overestimated by a factor of 2.5; although this was compensated by applying a correction to the response in temperature and residual circulation, the underlying hypothesis of linearity in the response might not be fully satisfied. On the other hand, the different climate sensitivities of the two models can lead to different response to ODS radiative forcing.

The third novel aspect of this study is the evaluation of the Antarctic ozone hole impact on the AoA, separating changes in residual circulation and mixing. This impact is largest in austral summer, and the results show very good agreement between reanalysis and model trends in that region and season. Antarctic ozone depletion accelerates the residual circulation (Figure 5), decreases lower stratospheric mixing, increases it at higher levels (Figure 8), and decreases AoA except in the lowermost polar stratosphere where AoA increases (Figure 9). Calculation of the RCTT and aging by mixing demonstrates that this AoA increase is due to reduced mixing associated with the delayed vortex breakup (Figure 11), as proposed recently by Li et al. (2018). While the aging by mixing trends in the lowermost stratosphere are strongly influenced by local mixing changes, at higher levels they are likely associated with changes in residual circulation. This is consistent with the conclusion of Dietmüller et al. (2017) that the contribution of local mixing to AoA is mainly limited to levels below 50 hPa. Moreover, this analysis shows a crucial role of aging by mixing for the global

trend patterns in AoA not only in DJF but also for the annual mean (Figures 10 and S1). Note that this not only includes changes in local mixing efficiency (shown here to drive AoA increases in the austral summer lower stratosphere), but mixing also acts as an amplifier of changes in the residual circulation (Garny et al., 2014; Ploeger et al., 2015). A potentially important caveat of this analysis is that the role of diffusive transport is not included in our analyses.

In summary, this work confirms a major role of increasing ODS concentrations on the BDC trends in recent decades and provides further insights on this influence by assessing the dominant role of ozone depletion and quantifying changes in AoA, residual circulation and mixing. We have focused on the period before 2000 because of the ODS increase until 2000. We therefore do not examine explicitly the cause of the weakening in the upwelling acceleration trend after the year 2000 derived from observations and reanalyses mentioned in the section 1. Nevertheless, in agreement with Polvani et al. (2018), we have shown that the ODS drive significant changes in upwelling, and thus the reduction of ODS in the 21st century is qualitatively consistent with a weakening of the upwelling trend.

Acknowledgments
We are thankful to Hella Garny for kindly providing the code to compute the RCTTs. M. A. acknowledges funding from the Program Atracción de Talento de la Comunidad de Madrid (2016-T2/AMB-1405), the Spanish National Projects STEADY (CGL2017-83198-R) and N.C. acknowledges PALEOSTRAT (CGL2015-69699), and the EU 7th framework Program under grant 603557 (StratoClim). This work has been carried out using the high performance computing and storage facilities provided by CISL/NCAR. F. P. was funded by the Helmholtz Association under grant VH-NG-1128 (Helmholtz Young Investigators Group A-SPECi). S. S. is partly supported by grant 133814 from the NSF. The WACCM data used here is available upon request to the authors. JRA-55 data are available at https://rda.ucar.edu/, and ERA-Interim data are available at http://apps.ecmwf.int/datasets/.

References

Abalos, M., Legras, B., Ploeger, F., & Randel, W. J. (2015). Evaluating the advective Brewer-Dobson circulation in three reanalyses for the period 1979–2012. *Journal of Geophysical Research: Atmospheres*, *120*, 7534–7554. https://doi.org/10.1002/2015JD023182

Abalos, M., Legras, B., & Shuckburgh, E. (2016). Interannual variability in effective diffusivity in the upper troposphere/lower stratosphere from reanalysis data. *Quarterly Journal of the Royal Meteorological Society*, *142*(697), 1847–1861. Retrieved from https://doi.org/10.1002/qj.2779

Aquila, V., Swartz, W. H., Waugh, D. W., Colarco, P. R., Pawson, S., Polvani, L. M., & Stolarski, R. S. (2016). Isolating the roles of different forcing agents in global stratospheric temperature changes using model integrations with incrementally added single forcings. *Journal of Geophysical Research: Atmospheres*, *121*, 8067–8082. https://doi.org/10.1002/2015JD023841

Aschmann, J., Burrows, J. P., Gebhardt, C., Rozanov, A., Hommel, R., Weber, M., & Thompson, A. M. (2014). On the hiatus in the acceleration of tropical upwelling since the beginning of the 21st century. *Atmospheric Chemistry and Physics*, *14*(23), 12,803–12,814. https://doi.org/10.5194/acp-14-12803-2014

Birner, T., & Bönisch, H. (2011). Residual circulation trajectories and transit times into the extratropical lowermost stratosphere. *Atmospheric Chemistry and Physics*, *11*(2), 817–827. https://doi.org/10.5194/acp-11-817-2011

Bönisch, H., Engel, A., Birner, T., Hoor, P., Tarasick, D. W., & Ray, E. A. (2011). On the structural changes in the Brewer-Dobson circulation after 2000. *Atmospheric Chemistry and Physics*, *11*(8), 3937–3948. https://doi.org/10.5194/acp-11-3937-2011

Butchart, N. (2014). The Brewer-Dobson circulation. *Reviews of Geophysics*, *52*, 157–184. https://doi.org/10.1002/2013RG000448

Chabrillat, S., Vigouroux, C., Christophe, Y., Engel, A., Errera, Q., Minganti, D., & Mahieu, E. (2018). Comparison of mean age of air in five reanalyses using the BASCOE transport model. *Atmospheric Chemistry and Physics*, *18*(19), 14,715–14,735. Retrieved from https://doi.org/10.5194/acp-18-14715-2018

de la Cámara, A., Lott, F., Jewtoukoff, V., Plougonven, R., & Hertzog, A. (2016). On the gravity wave forcing during the southern stratospheric final warming in LMDZ. *Journal of the Atmospheric Sciences*, *73*(8), 3213–3226. Retrieved from https://doi.org/10.1175/JAS-D-15-0377.1

Dee, D. P., Co-authors, Uppala, S. M., Simmons, A. J., Berrisford, P., Poli, P., & Vitart, F. (2011). The ERA-Interim reanalysis: Configuration and performance of the data assimilation system. *Quarterly Journal of the Royal Meteorological Society*, *137*(656), 553–597. https://doi.org/10.1002/qj.828

Diallo, M., Legras, B., & Chédin, A. (2012). Age of stratospheric air in the ERA-Interim. *Atmospheric Chemistry and Physics*, *12*(24), 12,133–12,154. https://doi.org/10.5194/acp-12-12133-2012

Dietmüller, S., Garny, H., Plöger, F., Jöckel, P., & Cai, D. (2017). Effects of mixing on resolved and unresolved scales on stratospheric age of air. *Atmospheric Chemistry and Physics*, *17*(12), 7703–7719. https://doi.org/10.5194/acp-17-7703-2017

Engel, A., Bönisch, H., Ullrich, M., Sitals, R., Membrive, O., Danis, F., & Crevoisier, C. (2017). Mean age of stratospheric air derived from AirCore observations. *Atmospheric Chemistry and Physics*, *17*(11), 6825–6838. https://doi.org/10.5194/acp-17-6825-2017

Engel, A., Möbius, T., Bönisch, H., Schmidt, U., Heinz, R., Levin, I., & Boering, K. (2009). Age of stratospheric air unchanged within uncertainties over the past 30 years. *Nature Geoscience*, *2*(1), 28–31. Retrieved from https://doi.org/10.1038/ngeo388

Eyring, V., Lamarque, J. F., Hess, P., Arfeuille, F., Bowman, K., Chipperfield, M. P., & Young, P. J. (2013). Overview of IGAC/SPARC Chemistry-Climate Model Initiative (CCMI) community simulations in support of upcoming ozone and climate assessments. *SPARC Newsletter*, *40*, 48–66.

Garcia, R. R., Kinnison, D. E., & Marsh, D. R. (2012). World avoided simulations with the Whole Atmosphere Community Climate Model. *Journal of Geophysical Research Atmospheres*, *117*, 1–16. https://doi.org/10.1029/2012JD018430

Garcia, R. R., Randel, W. J., & Kinnison, D. E. (2011). On the determination of age of air trends from atmospheric trace species. *Journal of the Atmospheric Sciences*, *68*(1), 139–154. Retrieved from https://doi.org/10.1175/2010JAS3527.1

Garcia, R. R., Smith, A. K., Kinnison, D. E., de la Cámara, Á., & Murphy, D. J. (2017). Modification of the gravity wave parameterization in the Whole Atmosphere Community Climate Model: Motivation and results. *Journal of the Atmospheric Sciences*, *74*(1), 275–291. https://doi.org/10.1175/JAS-D-16-0104.1

Garfinkel, C. I., Aquila, V., Waugh, D. W., & Oman, L. D. (2017). Time-varying changes in the simulated structure of the Brewer-Dobson Circulation. *Atmospheric Chemistry and Physics*, *17*(2), 1313–1327. https://doi.org/10.5194/acp-17-1313-2017

Garny, H., Birner, T., Bönisch, H. & Bunzel, F. (2014). The effects of mixing on age of air. *Journal of Geophysical Research: Atmospheres*, *119*, 7015–7034. https://doi.org/10.1002/2013JD021417

Haenel, F. J., Stiller, G. P., Von Clarmann, T., Funke, B., Eckert, E., Glatthor, N., & Reddmann, T. (2015). Reassessment of MIPAS age of air trends and variability. *Atmospheric Chemistry and Physics*, *15*(22), 13161–13176. https://doi.org/10.5194/acp-15-13161-2015

Hardiman, S. C., Lin, P., Scaife, A. A., Dunstone, N. J., & Ren, H. L. (2017). The influence of dynamical variability on the observed Brewer-Dobson circulation trend. *Geophysical Research Letters*, *44*, 2885–2892. https://doi.org/10.1002/2017GL072706

Haynes, P., & Shuckburgh, E. (2000). Effective diffusivity as a diagnostic of atmospheric transport: 1. Stratosphere. *Journal of Geophysical Research*, *105*(D18), 22777. Retrieved from https://doi.org/10.1029/2000JD900093

Hegglin, M. I., Plummer, D. A., Shepherd, T. G., Scinocca, J. F., Anderson, J., Froidevaux, L., & Weigel, K. (2014). Vertical structure of stratospheric water vapour trends derived from merged satellite data. *Nature Geoscience*, *7*(10), 768–776. https://doi.org/10.1038/NGEO2236

Keeble, J., Braesicke, P., Abraham, N. L., Roscoe, H. K., & Pyle, J. A. (2014). The impact of polar stratospheric ozone loss on Southern Hemisphere stratospheric circulation and climate. *Atmospheric Chemistry and Physics*, *14*(24), 13705–13717. Retrieved from https://doi.org/10.5194/acp-14-13705-2014

Khaykin, S. M., Funatsu, B. M., Hauchecorne, A., Godin-Beekmann, S., Claud, C., Keckhut, P., & Lauritsen, K. B. (2017). Postmillennium changes in stratospheric temperature consistently resolved by GPS radio occultation and AMSU observations. *Geophysical Research Letters*, *44*, 7510–7518. https://doi.org/10.1002/2017GL074353

Kinnison, D. E., Brasseur, G. P., Walters, S., Garcia, R. R., Marsh, D. R., Sassi, F., & Simmons, A. J. (2007). Sensitivity of chemical tracers to meteorological parameters in the MOZART-3 chemical transport model. *Journal of Geophysical Research*, *112*, D20302. Retrieved from https://doi.org/10.1029/2006JD007879

Kobayashi, S., Ota, Y., Harada, Y., Ebita, A., Moriya, M., Onoda, H., & Takahashi, K. (2015). The JRA-55 Reanalysis: General specifications and basic characteristics. *Journal of the Meteorological Society of Japan. Ser. II*, *93*(1), 5–48. Retrieved from https://doi.org/10.2151/jmsj.2015-001

Li, F., Austin, J., & Wilson, J. (2008). The strength of the Brewer-Dobson circulation in a changing climate: Coupled chemistry-climate model simulations. *Journal of Climate*, *21*(1), 40–57. https://doi.org/10.1175/2007JCLI1663.1

Li, F., Newman, P., Pawson, S., & Perlwitz, J. (2018). Effects of greenhouse gas increase and stratospheric ozone depletion on stratospheric mean age of air in 1960-2010. *Journal of Geophysical Research: Atmospheres*, *2010*, 2098–2110. Retrieved from https://doi.org/10.1002/2017JD027562

Mahieu, E., Chipperfield, M. P., Notholt, J., Reddmann, T., Anderson, J., Bernath, P. F., & Walker, K. A. (2014). Recent Northern Hemisphere stratospheric HCl increase due to atmospheric circulation changes. *Nature*, *515*(7525), 104–107. Retrieved from https://doi.org/10.1038/nature13857

Marsh, D. R., Mills, M. J., Kinnison, D. E., Lamarque, J. F., Calvo, N., & Polvani, L. M. (2013). Climate change from 1850 to 2005 simulated in CESM1 (WACCM). *Journal of Climate*, *26*(19), 7372–7391. https://doi.org/10.1175/JCLI-D-12-00558.1

McLandress, C., Jonsson, A. I., Plummer, D. A., Reader, M. C., Scinocca, J. F., & Shepherd, T. G. (2010). Separating the dynamical effects of climate change and ozone depletion. Part I: Southern Hemisphere stratosphere. *Journal of Climate*, *23*(18), 5002–5020. https://doi.org/10.1175/2010JCLI3586.1

McLandress, C., Shepherd, T. G., Reader, M. C., Plummer, D. A., & Shine, K. P. (2014). The climate impact of past changes in halocarbons and CO_2 in the tropical UTLS region. *Journal of Climate*, *27*(23), 8646–8660. https://doi.org/10.1175/JCLI-D-14-00232.1

Miyazaki, K., Iwasaki, T., Kawatani, Y., Kobayashi, C., Sugawara, S., & Hegglin, M. I. (2016). Inter-comparison of stratospheric mean-meridional circulation and eddy mixing among six reanalysis data sets. *Atmospheric Chemistry and Physics*, *16*(10), 6131–6152. https://doi.org/10.5194/acp-16-6131-2016

Molina, M. J., & Rowland, F. S. (1974). Stratospheric sink for chlorofluoromethanes: Chlorine atom-catalysed destruction of ozone. *Nature*, *249*(5460), 810–812. Retrieved from https://doi.org/10.1038/249810a0

Morgenstern, O., Hegglin, M. I., & Rozanov, E., O'Connor, F. M., Abraham, N. L., Akiyoshi, H., et al. (2017). Review of the global models used within phase 1 of the Chemistry-Climate Model Initiative (CCMI). *Geoscientific Model Development*, *10*, 639–671. https://doi.org/10.5194/gmd-10-639-2017

Morgenstern, O., Stone, K. A., Schofield, R., Akiyoshi, H., Yamashita, Y., Kinnison, D. E., & Chipperfield, M. P. (2018). Ozone sensitivity to varying greenhouse gases and ozone-depleting substances in CCMI-1 simulations. *Atmospheric Chemistry and Physics*, *18*(2), 1091–1114. https://doi.org/10.5194/acp-18-1091-2018

Myhre, G., & Shindell, D. (2013). Anthropogenic and natural radiative forcing. Climate Change 2013 the Physical Science Basis: Working Group I Contribution to the Fifth Assessment Report of the Intergovernmental Panel on Climate Change (Vol. 9781107057, pp. 659-740). https://doi.org/10.1017/CBO9781107415324.018

Neale, R. B., Richter, J., Park, S., Lauritzen, P. H., Vavrus, S. J., Rasch, P. J., & Zhang, M. (2013). The mean Climate of the Community Atmosphere Model (CAM4) in forced SST and fully coupled experiments. *Journal of Climate*, *26*(14), 5150–5168. https://doi.org/10.1175/JCLI-D-12-00236.1

Newman, P. A., Oman, L. D., Douglass, A. R., Fleming, E. L., Frith, S. M., Hurwitz, M. M., & Velders, G. J. (2009). What would have happened to the ozone layer if chlorofluorocarbons (CFCs) had not been regulated? *Atmospheric Chemistry and Physics*, *9*(6), 2113–2128. https://doi.org/10.5194/acp-9-2113-2009

Oberländer, S., Langematz, U., & Meul, S. (2013). Unraveling impact factors for future changes in the Brewer-Dobson circulation. *Journal of Geophysical Research: Atmospheres*, *118*, 10296–10312. https://doi.org/10.1002/jgrd.50775

Oberländer-Hayn, S., Meul, S., Langematz, U., Abalichin, J., & Haenel, F. (2015). A chemistry-climate model study of past changes in the Brewer-Dobson circulation. *Journal of Geophysical Research: Atmospheres*, *120*, 6742–6757. https://doi.org/10.1002/2014JD022843

Oman, L., Waugh, D. W., Pawson, S., Stolarski, R. S., & Newman, P. A. (2009). On the influence of anthropogenic forcings on changes in the stratospheric mean age. *Journal of Geophysical Research*, *114*, D03105. https://doi.org/10.1029/2008JD010378

Orr, A., Bracegirdle, T. J., Hosking, J. S., Feng, W., Roscoe, H. K., & Haigh, J. D. (2013). Strong dynamical modulation of the cooling of the polar stratosphere associated with the Antarctic ozone hole. *Journal of Climate*, *26*(2), 662–668. https://doi.org/10.1175/JCLI-D-12-00480.1

Ploeger, F., Abalos, M., Birner, T., Konopka, P., Legras, B., Müller, R., & Riese, M. (2015). Quantifying the effects of mixing and residual circulation on trends of stratospheric mean age of air. *Geophysical Research Letters*, *42*, 2047–2054. https://doi.org/10.1002/2014GL062927

Ploeger, F., & Birner, T. (2016). Seasonal and inter-annual variability of lower stratospheric age of air spectra. *Atmospheric Chemistry and Physics*, *16*(15), 10195–10213. https://doi.org/10.5194/acp-16-10195-2016

Plumb, R. A. (2002). Stratospheric transport. *Journal of the Meteorological Society of Japan*, *80*(4B), 793–809. Retrieved from https://doi.org/10.2151/jmsj.80.793

Polvani, L. M., Abalos, M., Garcia, R., Kinnison, D., & Randel, W. J. (2018). Significant weakening of Brewer-Dobson circulation trends over the 21st century as a consequence of the Montreal Protocol. *Geophysical Research Letters*, *45*, 401–409. Retrieved from https://doi.org/10.1002/2017GL075345

Polvani, L. M., Sun, L., Butler, A. H., Richter, J. H., & Deser, C. (2017). Distinguishing stratospheric sudden warmings from ENSO as key drivers of wintertime climate variability over the North Atlantic and Eurasia. *Journal of Climate*, *30*(6), 1959–1969. https://doi.org/10.1175/JCLI-D-16-0277.1

Previdi, M., & Polvani, L. M. (2014). Climate system response to stratospheric ozone depletion and recovery. *Quarterly Journal of the Royal Meteorological Society*, *140*(685), 2401–2419. https://doi.org/10.1002/qj.2330

Randel, W. J., Polvani, L., Wu, F., Kinnison, D. E., Zou, C. Z., & Mears, C. (2017). Troposphere-stratosphere temperature trends derived from satellite data compared with ensemble simulations from WACCM. *Journal of Geophysical Research: Atmospheres*, *122*, 9651–9667. https://doi.org/10.1002/2017JD027158

Ray, E. A., Moore, F. L., Rosenlof, K. H., Davis, S. M., Sweeney, C., Tans, P., & Aoki, S. (2014). Improving stratospheric transport trend analysis based on SF6 and CO2 measurements. *Journal of Geophysical Research: Atmospheres*, *119*, 14,110–14,128. https://doi.org/10.1002/2014JD021802

Solomon, S., Garcia, R. R., Rowland, F. S., & Wuebbles, D. J. (1986). On the depletion of Antarctic ozone. *Nature*, *321*(6072), 755–758. Retrieved from https://doi.org/10.1038/321755a0

Son, S. W., Gerber, E. P., Perlwitz, J., Polvani, L. M., Gillett, N. P., Seo, K. H., & Yamashita, Y. (2010). Impact of stratospheric ozone on Southern Hemisphere circulation change: A multimodel assessment. *Journal of Geophysical Research*, *115*, D00M07. https://doi.org/10.1029/2010JD014271

Solomon, S., Ivy, D. J., Kinnison, D., Mills, M. J., Neely, R. R., & Schmidt, A. (2016). Emergence of healing in the Antarctic ozone layer. *Science*, *353*(6296), 269–74. https://doi.org/10.1126/science.aae0061

Stiller, G. P., Fierli, F., Ploeger, F., Cagnazzo, C., Funke, B., Haenel, F. J., & Von Clarmann, T. (2017). Shift of subtropical transport barriers explains observed hemispheric asymmetry of decadal trends of age of air. *Atmospheric Chemistry and Physics*, *17*(18), 11172–11192. https://doi.org/10.5194/acp-17-11177-2017

Stiller, G. P., Von Clarmann, T., Haenel, F., Funke, B., Glatthor, N., Grabowski, U., & López-Puertas, M. (2012). Observed temporal evolution of global mean age of stratospheric air for the 2002 to 2010 period. *Atmospheric Chemistry and Physics*, *12*(7), 3311–3331. https://doi.org/10.5194/acp-12-3311-2012

Thompson, D. W. J., Solomon, S., Kushner, P. J., England, M. H., Grise, K. M., & Karoly, D. J. (2011). Signatures of the Antarctic ozone hole in Southern Hemisphere surface climate change. *Nature Geoscience*, *4*(11), 741–749. Retrieved from https://doi.org/10.1038/ngeo1296

Young, P. J., Rosenlof, K. H., Solomon, S., Sherwood, S. C., Fu, Q., & Lamarque, J. F. (2012). Changes in stratospheric temperatures and their implications for changes: In the Brewer-Dobson circulation, 1979-2005. *Journal of Climate*, *25*(5), 1759–1772. https://doi.org/10.1175/2011JCLI4048.1